Korean J. Chem. Eng., **28**(2), 364-369 (2011)
DOI: 10.1007/s11814-010-0416-z

Numerical simulation of bidisperse hard spheres settling in a fluid

Sangkyun Koo†

Department of Industrial Chemistry, Sangmyung University, Seoul 110-743, Korea
(*Received 19 July 2010 • accepted 29 August 2010*)

Abstract–Average settling velocity of non-uniform hard spheres in a viscous fluid is determined by using a large-scale numerical simulation that is carried out for over 10^3 spheres in a periodic unit cell which extends infinitely. An efficient calculation scheme is used for reducing the computation cost which steeply increases with the number of the spheres. The calculation scheme is based on a fast summation method for far-field hydrodynamic interaction among spheres. It is applied in the computation of hindered settling velocity of hard spheres with bidisperse size distribution in a viscous fluid. The simulation results are compared with the theoretical predictions by Batchelor [8] and Davis and Gecol [9]. It is found that the prediction by Davis and Gecol reasonably agrees with the numerical results.

Key words: Bidisperse Suspension, Hindered Settling Velocity, Fast Summation Algorithm, Stokes Flow Simulation, Multipole Expansion

INTRODUCTION

Stokes flow simulation technique for suspensions enables us to make particle-scale analysis of the suspensions and hence to understand their macroscopic behavior. It also provides a useful tool to investigate microstructural change of the suspension to the imposed macroscopic circumstances. Suspensions consist of suspended particles and surrounding fluid. The number of particles is nearly infinite and the particles are randomly distributed. Mathematically the suspension can be described as periodic extension of a representative unit cell containing particles. It is hoped to include as many particles as possible in the unit cell in order to simulate the suspensions more realistically. A large number of particles is necessary for the analysis of various phenomena occurring in suspensions. Bossis and Brady [1], for example, found the shear-induced agglomeration of particles in a suspension using 49 particles in a two-dimensional space. Inclusion of a large number of particles, however, requires heavy computation cost. The overall computation cost for the suspension simulation usually increases with the cubic power to the number of particles, N, and the computation is also limited by computer performance. Although much progress has been made in computer performance in recent decades, it is still challenging to carry out the simulation with a large number of particles over $O(10^3)$. An alternative to overcome the limit of computing capacity is to devise an efficient calculation method which reduces the computation cost. Recently, several investigators have proposed novel numerical schemes for the large scale simulation of suspensions [2-5]. Sangani and Mo [3] made significant progress in reducing computation cost with a fast summation technique for calculating far-field interaction of particles. They applied the concept of a fast algorithm for classical physics [6,7] to the Stokes flow simulations.

In the present study this fast summation algorithm is applied to the case of hard sphere suspensions with bidisperse size distribution of spherical particles. Specifically, the large-scale simulation method is used to determine the average settling velocity of the bidisperse suspensions when the Péclet number based on particle motion is large and the densities of particles are uniform. Sedimentation processes are widely utilized in particle-fluid separation for suspensions and slurries, particle fractionation in size or density of the particles, and colloidal crystallization. The theory for the sedimentation process also provides an analytical tool for evaluating dispersion stability of colloidal solutions or suspensions. Size distribution of suspended particles is one of the important factors determining transport properties of the suspensions. Due to the practical and theoretical significance, there have been numerous studies on the sedimentation of the bidisperse suspensions [8-14]. However, particle-scale numerical simulation with a large number of particles over 10^3 is seldom found for the Stokes flow in bidisperse suspensions. The present work provides the calculation results for average sedimentation velocity of bidisperse suspensions. The results are compared with theoretical predictions by Batchelor and Wen [8] and Davis and Gecol [9].

†To whom correspondence should be addressed.
E-mail: skkoo@smu.ac.kr

THEORY AND NUMERICAL METHOD

1. Theory

We consider a Stokes flow around N spherical particles in a unit cell which extends periodically throughout unbounded space. The fluid flow satisfies Stokes equation with a point force $\mathbf{f}_i$ at the lattice point of the periodic unit cell,

$$-\nabla p + \eta \nabla^2 \mathbf{u}_i = \sum_{\mathbf{x}_L} \mathbf{f}_i \delta(\mathbf{x} - \mathbf{x}_L), \tag{1}$$

and the continuity equation,

$$\nabla \cdot \mathbf{u}_i = 0. \tag{2}$$

Here the notations p, $\mathbf{u}_i$, η, δ and $\mathbf{x}$ are the pressure in the fluid, the fluid velocity, the fluid viscosity, the delta function, and the position vector, respectively. And $\mathbf{x}_L$ denotes the position vector for the lattice point. The solution of these equations is given by Green function M_{ij}

$$u_i(\mathbf{x})=M_{ij}(\mathbf{x})\cdot F_j, \tag{3}$$

where

$$F_j=f_j/(-4\pi\eta). \tag{4}$$

The Green function M_{ij} is written in terms of the spatially periodic fundamental solutions S_1 and S_2

$$M_{ij}(\mathbf{x})=S_1(\mathbf{x})\delta_{ij}-\frac{\partial^2 S_2(\mathbf{x})}{\partial x_i \partial x_j}, \tag{5}$$

where

$$S_m(\mathbf{x})=\frac{(-4\pi^2)^{1-m}}{\pi\tau}\sum_{\mathbf{k}\neq\mathbf{0}} k^{-2m}\exp(-2\pi i\mathbf{k}\cdot\mathbf{x}),\ \ m=1,2 \tag{6}$$

and τ is the volume of the unit cell and $\mathbf{k}$ is the reciprocal lattice vector. Using the properties of the Green function, we obtain the general solution of the equations as follows.

$$u_i(\mathbf{x})=U_i^{\infty}(\mathbf{x})+\sum_{\alpha=1}^{N}\mathscr{D}_j^{\alpha}M_{ij}(\mathbf{x}-\mathbf{x}^{\alpha}) \tag{7}$$

$$\mathscr{D}_j^{\alpha}=A_j^{\alpha}+B_{jk}^{\alpha}\partial_k+C_{jkl}^{\alpha}\partial_{kl}^2+\cdots \tag{8}$$

Here, U_i^{∞} is the mean velocity of fluid due to the imposed flow and $\mathscr{D}_j^{\alpha}$ is the differential operator. The coefficients A_j^{α}, B_{jk}^{α}, and C_{jkl}^{α} are called the multipoles and are directly related to the force, torque, and stresslet acting on the spheres, respectively.

The present study follows a multipole expansion method developed by Mo and Sangani [15] who made use of Lamb's general solution for Stokes flow around spheres. Lamb's general solution around a sphere α is given by [16]

$$\mathbf{u}(\mathbf{x})=\sum_{n=-\infty}^{\infty}\left[\left(\frac{n+3}{2(n+1)(2n+3)}r^2\nabla p_n^{\alpha}-\frac{n}{(n+1)(2n+3)}\mathbf{r}p_n^{\alpha}\right)+\nabla\times(\mathbf{r}\chi_n^{\alpha})+\nabla\Phi_n^{\alpha}\right], \tag{9}$$

where $\mathbf{r}=\mathbf{x}-\mathbf{x}^{\alpha}$ and p_n^{α}, χ_n^{α}, are Φ_n^{α} the n^{th} order spherical harmonics. At r=0, i.e., $\mathbf{x}=\mathbf{x}^{\alpha}$, the negative order of the harmonics is singular, whereas the non-negative order harmonics is regular. Hence the harmonics p_n^{α} are expressed by the sum of its singular part,

$$p_{-n-1}^{s,\alpha}=\sum_{m=0}^{n}p_n^m(\cos\theta)(P_{nm}^{s,\alpha}\cos m\varphi+\tilde{P}_{nm}^{s,\alpha}\sin m\varphi)r^{-n-1}\quad (n>0), \tag{10}$$

and regular part,

$$p_n^{r,\alpha}=\sum_{m=0}^{n}p_n^m(\cos\theta)(P_{nm}^{r,\alpha}\cos m\varphi+\tilde{P}_{nm}^{r,\alpha}\sin m\varphi)r^{n}\quad (n\geq 0), \tag{11}$$

where $P_{nm}^{s,\alpha}$ and $\tilde{P}_{nm}^{s,\alpha}$ are the coefficients of singular harmonics and likewise $P_{nm}^{r,\alpha}$ and $\tilde{P}_{nm}^{r,\alpha}$ are the coefficients of regular harmonics. The function P_n^m is the associated Legendre polynomial with θ and φ being the polar and azimuthal angle each for the spherical polar coordinate when $\mathbf{x}^{\alpha}$ and axis are taken as origin and polar axis, respectively. Similarly, χ_n^{α} and Φ_n^{α} are also given in terms of the corresponding coefficients as follows.

$$\chi_{-n-1}^{s,\alpha}=\sum_{m=0}^{n}p_n^m(\cos\theta)(T_{nm}^{s,\alpha}\cos m\varphi+\tilde{T}_{nm}^{s,\alpha}\sin m\varphi)r^{-n-1}\quad (n>0),$$

$$\chi_n^{r,\alpha}=\sum_{m=0}^{n}p_n^m(\cos\theta)(T_{nm}^{r,\alpha}\cos m\varphi+\tilde{T}_{nm}^{r,\alpha}\sin m\varphi)r^{n}\quad (n\geq 0),$$

$$\Phi_{-n-1}^{s,\alpha}=\sum_{m=0}^{n}p_n^m(\cos\theta)(\Psi_{nm}^{s,\alpha}\cos m\varphi+\tilde{\Psi}_{nm}^{s,\alpha}\sin m\varphi)r^{-n-1}\quad (n\geq 0),$$

$$\Phi_n^{r,\alpha}=\sum_{m=0}^{n}p_n^m(\cos\theta)(\Psi_{nm}^{r,\alpha}\cos m\varphi+\tilde{\Psi}_{nm}^{r,\alpha}\sin m\varphi)r^{n}\quad (n\geq 0). \tag{12}$$

Here $T_{nm}^{s,\alpha}$, $\tilde{T}_{nm}^{s,\alpha}$, $\Psi_{nm}^{s,\alpha}$, are $\tilde{\Psi}_{nm}^{s,\alpha}$ the singular coefficients and $T_{nm}^{r,\alpha}$, $\tilde{T}_{nm}^{r,\alpha}$, $\Psi_{nm}^{r,\alpha}$, are $\tilde{\Psi}_{nm}^{r,\alpha}$ are the regular coefficients.

Lamb's general solutions can be related to the multipoles. The singular and regular coefficients of Lamb's solutions are matched to the corresponding multipoles. Kim and Karilla [17] and Mo and Sangani [15] gave the relation between Lamb's solutions and the multipoles. We follow Mo and Sangani [15]. The singular part of the velocity at $\mathbf{x}$, $u_i^{\alpha,s}(\mathbf{x})$, is written by

$$u_i^{\alpha,s}(\mathbf{x})=\mathscr{D}^{\alpha}M_{ij}^{\alpha,s}(\mathbf{x}), \tag{13}$$

where the superscript s denotes the singular solution. And the regular coefficients at $\mathbf{x}^{\alpha}$ is written in terms of the singular coefficients of the other spheres. For example $P_{nm}^{\alpha,r}$ is given by

$$P_{mm}^{\alpha,r}=\frac{(-2)^m}{(1+\delta_{m0})(n+m)!}\sum_{\beta=1}^{N}[\mathscr{L}_n^m(\mathbf{x}\cdot\mathscr{H}^{\beta}\nabla^2-\nabla\cdot\mathscr{H}^{\beta})]S_1(\mathbf{x}^{\alpha}-\mathbf{x}^{\beta}), \tag{14}$$

where $\mathscr{L}_n^m$ is the differential operator defined by the following Eqs. (15)-(17) [20]

$$\mathscr{L}_n^m=\frac{\partial^{n-m}}{\partial x_1^{n-m}}\Delta_m,\quad \tilde{\mathscr{L}}_n^m=\frac{\partial^{n-m}}{\partial x_1^{n-m}}\tilde{\Delta}_m \tag{15}$$

$$\Delta_m=\frac{\partial^m}{\partial\xi}+\frac{\partial^m}{\partial\upsilon},\quad \tilde{\Delta}_m=i\left(\frac{\partial^m}{\partial\xi}-\frac{\partial^m}{\partial\upsilon}\right) \tag{16}$$

$$\xi=x_2+ix_3,\ \upsilon=x_2-ix_3. \tag{17}$$

And $\mathscr{H}^{\beta}$ is a differential operator which is expressed in terms of the singular coefficients $P_{nm}^{s,\alpha}$, $\tilde{P}_{nm}^{s,\alpha}$, $T_{nm}^{s,\alpha}$, $\tilde{T}_{nm}^{s,\alpha}$. Writing one component of $\mathscr{H}^{\beta}$,

$$\mathscr{H}_1^{\beta}=\sum_{n=1}^{\infty}\sum_{m=0}^{n}\frac{2^{m-1}m}{(-1)^{n-m}(n-m)!}\{(-\tilde{T}_{nm}^{s,\alpha}\mathscr{L}_n^m+T_{nm}^{s,\alpha}\tilde{\mathscr{L}}_n^m)-\frac{(n-m)(n+m)}{nm(2n-1)}(P_{nm}^{s,\alpha}\mathscr{L}_n^m+\tilde{P}_{nm}^{s,\alpha}\tilde{\mathscr{L}}_n^m)\}. \tag{18}$$

The other components of $\mathscr{H}^{\beta}$ are also similarly given. Therefore, in order to determine $P_{nm}^{\alpha,r}$ we need to evaluate Green's function $S_1(\mathbf{x}^{\alpha}-\mathbf{x}^{\beta})$ and its differentiation. This is a very complicated calculation which takes high computation cost. Therefore, the computation load for this part should be reduced in order to perform large scale Stokes flow simulations for suspensions.

2. Fast Summation Method

Since the numerical computation of hydrodynamic interactions among the spheres is carried out in pairwise manner, the computation cost rapidly increases with the number of particles. To reduce the computation cost, an efficient method for calculating the far-field hydrodynamic interactions among spheres is introduced. This method employs a fast summation method based on hierarchical grouping of spheres at large distance from the sphere at origin. The idea is that the multipoles due to the spheres in a certain region far from the position considered as origin are translated to the corresponding multipoles of the center of the region, and the translated multipoles from each sphere at the region are summed. Hence, the

overall interactions from the spheres in that region are represented by the translated multipoles. Then we can avoid the pairwise calculation between the spheres far apart and thus the computation cost is much reduced.

For the grouping the cubic structure of the unit cell is virtually subdivided in proportion to the number of spheres. The subdivision is performed so that the number of spheres in the smallest sub-cell be O(1). If the unit cell is subdivided once in each direction, 64 sub-cells are formed. This is the coarsest level. As the number of spheres increases, we subdivide more and then a larger number of sub-cells are formed. Hence, a hierarchical tree structure is built in a unit cell, which depends on the degree of subdivision. The fast summation starts from individual spheres to the center of the sub-cell at the lowest degree of subdivision, in which the individual spheres are located. We make use of Green's identity for the translation of multipoles,

$$\int_V (\zeta\nabla^2\psi-\psi\nabla^2\zeta)\mathrm{dV}=\int_{\partial V}(\zeta\nabla\psi-\psi\nabla\zeta)\cdot\mathbf{n}\mathrm{dA}. \tag{19}$$

Assuming a volume V including two positions on the surface of the volume, the translation of the multipoles between the two becomes relatively simple when harmonic and biharmonic functions are used as ζ and ψ in Eq. (19). The two positions can be taken as those for a sphere and the center in the region where the sphere and its neighbors are located. For example, the singular coefficient $P_{nm}^{\alpha,s}$ for the sphere can be translated to that for the center of the region as follows:

$$P_{nm}^{i,coarse}=\frac{2(-1)^n(n-m)!}{(1+\delta_{m0})(n+m)!}\sum_{k=1}^{\infty}\sum_{l=0}^{k}\sum_{i=1}^{N_f}\frac{(2)^{1-l}}{(-1)^{k-l}(k-1)!}$$
$$P_{kl}^{i,fine}\mathscr{L}_k^{l,i}Y_{nm}^{j}(\mathbf{x}^{\boldsymbol{coarse}}-\mathbf{x}^{\boldsymbol{fine}}), \tag{20}$$

where the superscripts 'coarse' and 'fine' denote the center of the region and the sphere, respectively, in this case. And N_f at the third summation is the number of spheres in the region. Other singular coefficients are similarly translated [3]. The translation of singular coefficients is continued until the singular coefficients at the all levels from individual spheres to the largest sub-cell are determined. The translation of regular coefficients is performed in the reverse way, that is, the way from the center of the region to the sphere.

Overall calculation scheme begins with taking initial guesses for the singular coefficients of individual spheres. The next is to translate the singular coefficients for fine levels to those for coarse levels until the singular coefficients at all levels are given. Then use is made for these singular coefficients to calculate the regular coefficients using the relations such as Eqs. (14)-(18). This calculation is first carried out in the lowest level. For the other finer levels we carry out both equal level calculation and translation of regular coefficients from the coarse level. Hence, the regular coefficients are expressed by the sum of translated coefficients and those for the equal level calculation. Through this scheme the singular and regular coefficients for all the levels are given and utilized for far-field calculation. These coefficients are rearranged to form a set of linear equations $\mathbf{A}\cdot\mathbf{x}=\mathbf{b}$ satisfying the boundary conditions.

To apply the boundary conditions at the surface of each sphere it is convenient to use u_r, $\nabla_s\cdot\mathbf{u}_s$, $\mathbf{e}_r\cdot(\nabla\times\mathbf{u}_s)$. Here u_r is the radial component of the velocity and $\mathbf{u}_s=u_\theta\mathbf{e}_\theta+u_\varphi\mathbf{e}_\varphi$ is the tangential velocity at the surface of sphere. And

$$\nabla=\mathbf{e}_r\frac{\partial}{\partial r}+\frac{1}{r}\nabla_s. \tag{21}$$

We can expand these three terms in spherical surface harmonics. For example, u_r is written as

$$u_r=\sum_{n=1}^{\infty}\sum_{m=0}^{n}((u_r)_{nm}Y_{nm}+(\tilde{u}_r)_{nm}\tilde{Y}_{nm}). \tag{22}$$

Similar expressions are obtained for $\nabla_s\cdot\mathbf{u}_s$ and $\mathbf{e}_r\cdot(\nabla\times\mathbf{u}_s)$. Combining these expressions to the singular and regular coefficients in Eqs. (9)-(12), we have

$$\Psi_{nm}^{r,\alpha}+\frac{(n+1)a^{-2n+1}}{n(2n-1)(2n+1)}P_{nm}^{s,\alpha}+\frac{a^2}{2(2n+1)}P_{nm}^{r,\alpha}=\frac{n(u_r)_{nm}-(\nabla\cdot u_s)_{nm}}{n(2n+1)a^{n-1}} \tag{23}$$

$$\Psi_{nm}^{s,\alpha}+\frac{a^2}{2(2n+1)}P_{nm}^{s,\alpha}+\frac{na^{2n+3}}{(n+1)(2n+1)(2n+3)}P_{nm}^{r,\alpha}$$
$$=\frac{-((n+1)(u_r)_{nm}+(\nabla\cdot\mathbf{u}_s)_{nm})}{(n+2)(2n+1)a^{-n-2}}, \tag{24}$$

$$T_{nm}^{r,\alpha}+T_{nm}^{s,\alpha}a^{-2n-1}=\frac{(\mathbf{e}_r\cdot(\nabla\times\mathbf{u}_s))_{nm}}{n(n+1)a^n}, \tag{25}$$

The right hand sides of Eqs. (23)-(25) are given by the imposed flow. Similar equations are given for the coefficients of $\tilde{Y}_{nm}$. For the sedimentation problem, these equations are supplemented by 3 N equations for the force acting on the sphere

$$\mathbf{F}^{\boldsymbol{reg}}+\mathbf{F}^{\boldsymbol{ext}}=0, \tag{26}$$

where $\mathbf{F}^{\boldsymbol{reg}}$ is the regular part of force evaluated at the center of the sphere, which is related to the singular coefficients, P_{1m}^s [15].

$$F_1^{reg}=-4\pi\eta P_{10}^s,$$
$$F_2^{reg}=4\pi\eta P_{11}^s, \tag{27}$$
$$F_3^{reg}=4\pi\eta\tilde{P}_{11}^s,$$

And $\mathbf{F}^{\boldsymbol{ext}}$ is the external force due to gravity for sedimentation problem. Similar relations can be used for the torque on the spheres. Eqs. (23)-(26) need to be truncated properly to form a finite number of linear equations. We follow the truncation scheme suggested by Mo and Sangani [15]. Hence in Eq. (23) $n\le n_s$, in Eq. (24) $n\le n_s-2$, and in Eq. (25) $n\le n_s-1$. Then we finally solve the set of linear equations to determine the singular coefficients and hence the multipoles for each sphere. The computation is iteratively performed until the singular coefficients converge. A generalized minimum residual method (GMRES) is used as a matrix solver. With these coefficients we determine the macroscopic transport properties of the process, such as the sedimentation velocity.

In addition to the fast summation technique, message passing interface (MPI) which is a parallel programming technique is implemented to reduce calculation time. Since the computation load should be distributed to multiprocessors performing the allocated part of the overall computations in parallel manner, the supercomputer facility (IBM machine) at Korea Institute of Science and Technology Information is used for the present study.

RESULTS AND DISCUSSION

First, we need to check the accuracy of the numerical calculation. Since we use an iterative method to solve $\mathbf{A}\cdot\mathbf{x}=\mathbf{b}$ for Eqs. (23)-

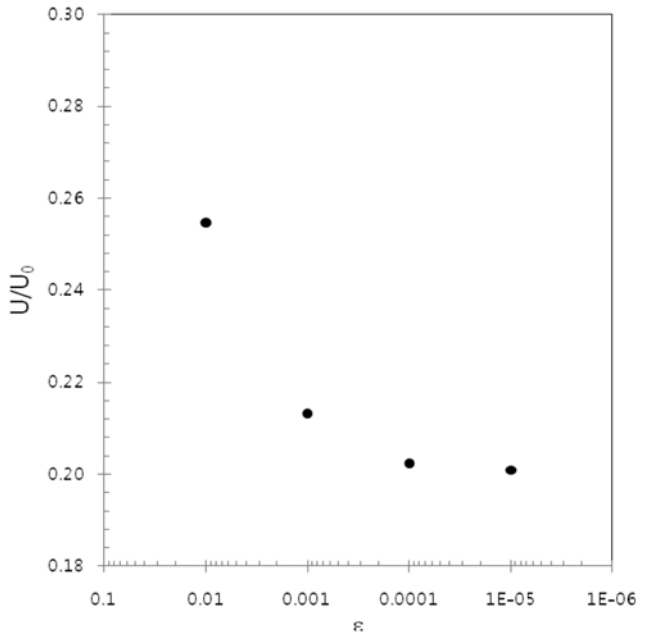

Fig. 1. Convergence of calculation results for sedimentation velocity with error tolerance ε.

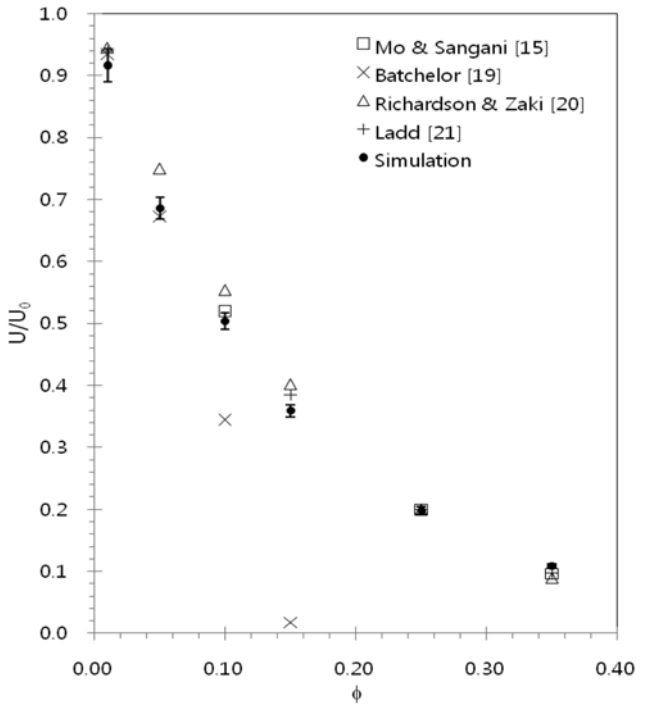

Fig. 2. Normalized average sedimentation velocity as a function of ϕ for monodisperse suspensions.

(26), we need to choose the tolerance e of error properly. The error is defined as

$$\text{error}=\left(\frac{\|\mathbf{b}-\mathbf{A}\cdot\mathbf{x}\|}{\|\mathbf{b}\|}\right)^{1/2}<\varepsilon, \tag{28}$$

where $\|\ \|$ is the Euclidean norm of the corresponding matrix. Fig. 1 shows normalized hindered settling velocity at four different values of the tolerance e from 0.01 to 0.00001 for a fixed configuration of monodisperse suspension at the particle volume fraction of ϕ=0.25 with the number of particles N=1,024. It is seen that the tolerance of 0.0001 is satisfactory. The calculation is carried out with the tolerance of 0.0001.

For proper truncation of the multipoles, we use two orders of the multipoles, n_s and n_t. The order n_t corresponds to the order of the multipoles for the translation of multipoles, whereas n_s is that for overall calculation. Table 1 shows the calculation results for hindered settling velocity for ϕ=0.25 and N=1,024, which vary with truncation. For n_s=2 and 3, n_t varies from n_t=n_s to n_t=n_s+2. The case of n_s=2 is seen less accurate. The converged value of the settling velocity is obtained beyond n_s=3 and n_t=3 and thus n_s=3 and n_t=5 are taken for the numerical calculation. Similar behavior is observed for a bidisperse suspension.

Table 1. Hindered settling velocity vs. truncation orders for monodisperse and bidisperse suspension

n	n_t	Monodisperse case	Bidisperse case	
		U*	U_1*	U_2*
2	2	0.2226	0.2868	0.0023
	3	0.2153	0.2506	0.0095
	4	0.2387	0.2604	0.0158
3	3	0.1726	0.2194	−0.0028
	4	0.2067	0.2323	0.0063
	5	0.2035	0.2324	0.0055
	6	0.2010	0.2321	0.0048

The hindered settling velocity (*) is the relative value to the Stokes velocity of large particle

With the truncation and tolerance determined, we calculate sedimentation velocity of monodisperse suspensions. The calculation is performed for 20 random arrays of 1,024 spheres for various concentrations. The random arrays of the spheres were generated by using a molecular dynamics code. The results are compared with those of the previous work in Fig. 2. The previous work includes theoretical predictions by Batchelor [19], empirical relation by Richardson-Zaki [20] and numerical calculation results by Mo and Sangani [15] and Ladd [21]. The well-known Batchelor's theory [19], which gives the linear relation between sedimentation velocity and concentration, holds for very dilute suspensions:

$$U=U_0(1-6.55\phi). \tag{29}$$

The Richardson-Zaki correlation is given by

$$U=U_0(1-\phi)^p \tag{30}$$

The power p in Eq. (30) is 4.7 in Richardson and Zaki's original work [20]. However, we use p=5.6 since the value p=5.6 is related to Davis and Gecol's formula [9] for bidisperse suspension. Fig. 2 shows that the predictions by Eq. (30) with p=5.6 agrees with numerical simulation results at ϕ=0.01. However Eq. (30) slightly overpredicts up to near ϕ=0.15 and then again agrees well with the simulations at ϕ=0.25 and 0.35. The simulation results by present work are in good agreement with those by Mo and Sangani [15] and Ladd [21].

For bidisperse suspensions, we put 1024 (or 1026) particles in

the unit cell. The size ratio λ is defined as the radius of small particles (a_2) to that of the large ones (a_1). Two size ratios were chosen: λ= 0.5 and 0.75. For both cases, the volume fraction of each species is chosen to be the half of the overall volume fraction ϕ which ranges 0.01 to 0.25. Figs. 3 and 4 show the simulation results for the normalized hindered settling velocities of large and small species for λ= 0.5. These results are compared with theoretical prediction by Batchelor and Wen [8] and semi-analytical estimation by Davis and Gecol [9]. Batchelor and Wen's theory [8] is given by

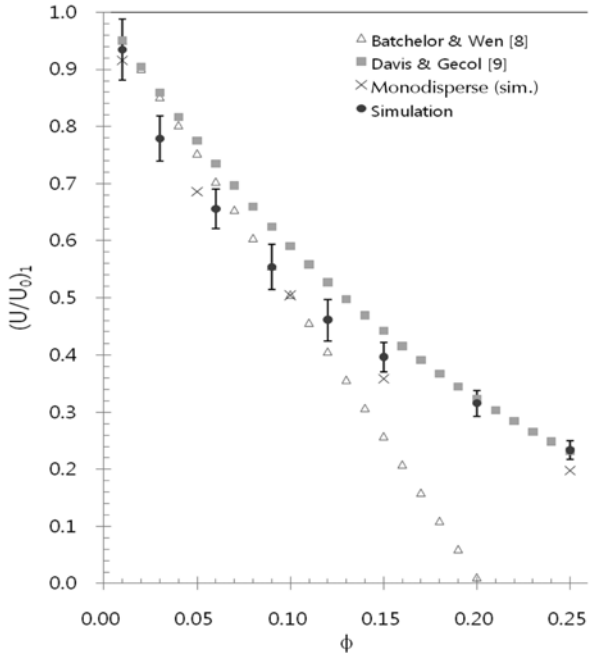

Fig. 3. $(U/U_0)_1$ as a function of ϕ for bidisperse suspensions. λ=0.5 and $\phi_1=\phi_2=\phi/2$.

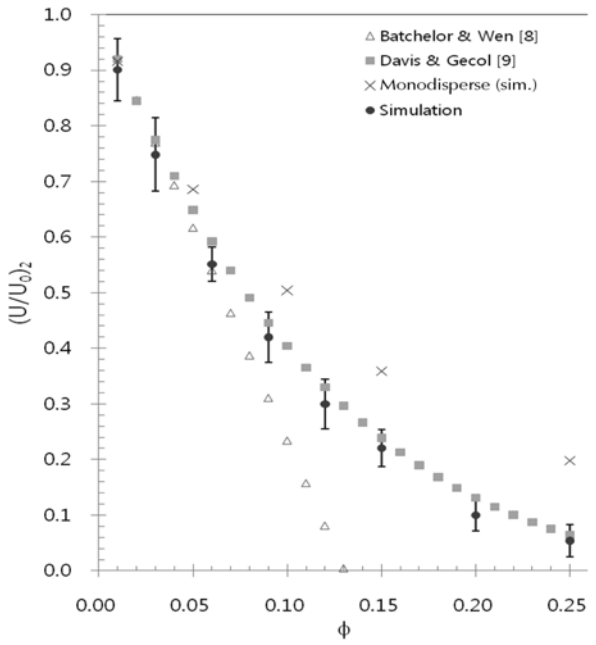

Fig. 4. $(U/U_0)_2$ as a function of ϕ for bidisperse suspensions. λ=0.5 and $\phi_1=\phi_2=\phi/2$.

$$U_i = U_{i,0}\left(1+\sum_{j=1}^{n} S_{ij}\phi_j\right), \tag{31}$$

where U_i and $U_{i,0}$ are the average settling velocity and the Stokes velocity of the species i, respectively. And S_{ij} is the sedimentation coefficient which depends on the size ratio of the species, volume fractions of each species, density ratio of the species, and Péclet number Pe based on the motion of the spherical particle. Since we are considering the case that densities of the species are equal and Pe is very large, i.e., Pe$\rightarrow\infty$, the sedimentation coefficient is given by

$$S_{ij} = -3.52 - 1.04\lambda - 1.03\lambda^2. \tag{32}$$

Eqs. (31) and (32) can be extended to the polydisperse case; however, these equations are for very dilute suspensions where hydrodynamic interaction is negligibly weak. Davis and Gecol [9] modified Eq. (31) by Batchelor and Wen [8] in order to extend its applicability to concentrate suspensions. The formula by Davis and Gecol is given by

$$U_i = U_{i,0}(1-\phi)^{-S_{ii}}\left(1+\sum_{j\neq i}^{n}(S_{ij}-S_{ii})\phi_j\right), \tag{33}$$

In Eq. (33), the term $(1-\phi)^{-S_{ii}}$ which is similar to Richardson-Zaki's empirical relation is introduced, giving nonlinearity with the concentration of suspension. We see that in very dilute limit Eq. (33) follows Batchelor and Wen's theory. Good agreement between the predictions by the two relations is found in both Figs. 3 and 4 at ϕ=0.01. However, it is seen that Eq. (33) gives slightly larger values of the normalized sedimentation velocity of large particle than the simulation does from ϕ=0.03 to 0.15, as shown in Fig. 3. Deviation of the predictions by Eq. (33) from the simulation results is within the error of 10%, considering the standard deviation of the simulation results. Beyond this regime, i.e., at ϕ=0.2 and 0.25, the prediction by Eq. (33) and the simulation results are in excellent agreement. Similar trend is observed in the case of monodisperse suspensions

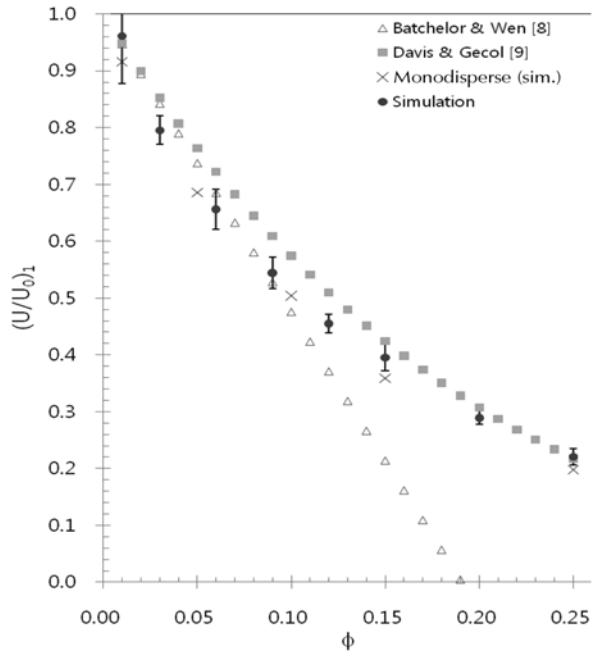

Fig. 5. $(U/U_0)_1$ as a function of ϕ for bidisperse suspensions. λ=0.75 and $\phi_1=\phi_2=\phi/2$.

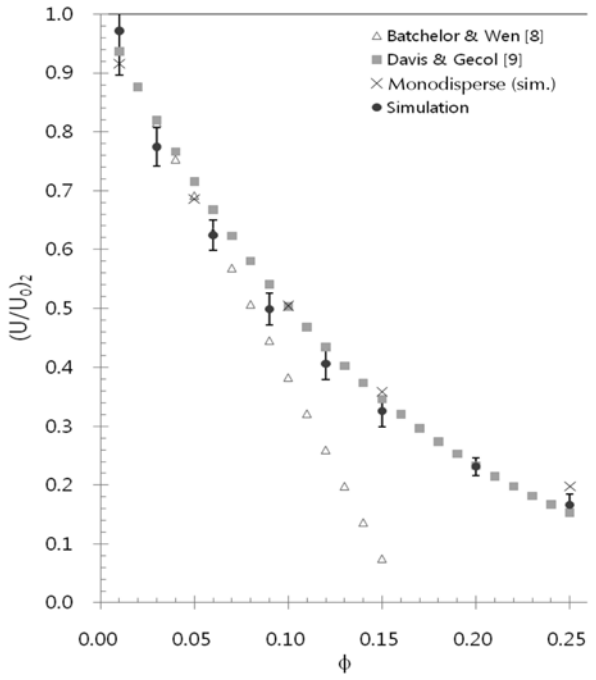

Fig. 6. $(U/U_0)_2$ as a function of ϕ for bidisperse suspensions. λ=0.75 and $\phi_1=\phi_2=\phi/2$.

and small particles in bidisperse suspension in Fig. 4. However, the prediction by Eq. (33) for the sedimentation velocity of small particles is within the range of the simulation results. We also find similar results for the case of λ=0.75 in Fig. 5 and 6. Overall, it is concluded that the predictions by Davis and Gecol [9] are in reasonable agreement with the numerical simulations.

SUMMARY

This paper dealt with numerical simulation for determining the velocity of non-uniform hard spheres settling through a Newtonian fluid. It is assumed that the Reynolds number based on average diameter of the spherical particles is less than unity and the particle Péclet number is very large. The spherical particles are of bidisperse size distribution. An efficient calculation scheme is used in the numerical simulation, which is based on a fast summation method for calculating far-field hydrodynamic interaction among the particles. The numerical simulation results show the average hindered settling velocity of bidisperse suspensions with more than 10^3 randomly placed particles over 20 configurations. These results are compared with the theoretical predictions by Batchelor and Wen [8] and Davis and Gecol [9]. The semi-analytical relation by Davis and Gecol follows Batchelor and Wen's theory at very dilute concentrations and its predictions for the average sedimentation velocity are in reasonable agreement with the numerical simulations.

ACKNOWLEDGEMENT

This work was supported by National Research Foundation of Korea Grant funded by the Korean Government (D 00115). Computations were performed using the supercomputer facilities provided by Korea Institute of Science and Technology Information.

NOMENCLATURE

a : radius of particle
F : force acting on particle
F_j : force acting on particle
f_j : point force at the lattice point of the unit cell
k : reciprocal lattice vector
M_{ij} : Oseen tensor (Green's function)
p : pressure
r : radial distance from the center of the particle at origin
S_1 : spatially periodic fundamental solution
S_2 : spatially periodic fundamental solution, $\nabla^2 S_2 = S_1$
S_{ij} : sedimentation coefficient
U : hindered settling velocity of particles in a fluid.
U_0 : settling velocity of an isolated particle in a fluid
$(U/U_0)_1$: normalized sedimentation velocity of large particles
$(U/U_0)_2$: normalized sedimentation velocity of small particles
u_i : velocity of the fluid (Einstein notation)
u : velocity of the fluid
x : position vector
$\mathbf{x}_L$: position vector for the lattice point of the unit cell

Greek Letters

ϕ : volume fraction of particles
η : viscosity of fluid
λ : size ratio of small to large particle
τ : volume of unit cell

REFERENCES

1. G. Bossis and J. F. Brady, *J. Chem. Phys*., **80**, 5141 (1984).
2. J. F. Brady and G. Bossis, *Annu. Rev. Fluid Mech*., **20**, 111 (1988).
3. A. S. Sangani and G. Mo, *Phys. Fluids*, **8**, 1990 (1996).
4. A. Sieru and J. F. Brady, *J. Fluid Mech*., **448**, 115 (2001).
5. A. J. Banchio and J. F. Brady, *J. Chem. Phys.*, **118**, 10323 (2003).
6. L. Greengard and V. Rokhlin, *J. Compu. Phys*., **73**, 325 (1987).
7. L. Greengard, *Science*, **265**, 909 (1994).
8. G. K. Batchelor and C. S. Wen, *J. Fluid Mech*., **124**, 495 (1982).
9. R. H. Davis and H. Gecol, *AIChE J*., **40**, 570 (1994).
10. M. K. Cheung, R. L. Powell and M. J. McCarthy, *AIChE J*., **42**, 271 (1996).
11. S. Koo and A. S. Sangani, *Phys. Fluids*, **14**, 3522 (2002).
12. M. Abbas, E. Climent, O. Simonin and M. R. Maxey, *Phys. Fluids*, **18**, 121504 (2006).
13. S. Koo, *J. Ind. Eng. Chem*., **14**, 679 (2009).
14. R. Dorell and A. J. Hogg, *Int. J. Multiphase Flow*, **36**, 481 (2010).
15. G. Mo and A. S. Sangani, *Phys. Fluids*, **6**, 1637 (1994).
16. H. Lamb, *Hydrodynamics*, Dover, New York (1945).
17. S. Kim and S. J. Karrila, *Microhydrodynamics*, Butterworth-Heinemann, Boston (1991).
18. E. W. Hobson, *The theory of spherical and ellipsoidal harmonics*, Cambridge University Press, Cambridge (1931).
19. G. K. Batchelor , *J. Fluid Mech*., **52**, 245 (1972).
20. J. F. Richadson and W. N. Zaki, *Trans. Inst. Chem. Eng.*, **32**, 35 (1954).
21. A. C. Ladd, *J. Chem. Phys*., **93**, 3484 (1990).